Mutation of a Single Residue in the S2–S3 Loop of CNG Channels Alters the Gating Properties and Sensitivity to Inhibitors

Jennifer I. Crary, Dylan M. Dean, Farahnaz Maroof, and Anita L. Zimmerman

From the Department of Molecular Pharmacology, Physiology and Biotechnology, Brown University, Providence, Rhode Island 02912

ABSTRACT We previously found that native cyclic nucleotide–gated (CNG) cation channels from amphibian rod cells are directly and reversibly inhibited by analogues of diacylglycerol (DAG), but little is known about the mechanism of this inhibition. We recently determined that, at saturating cGMP concentrations, DAG completely inhibits cloned bovine rod (Brod) CNG channels while only partially inhibiting cloned rat olfactory (Rolf) channels (Crary, J.I., D.M. Dean, W. Nguitragool, P.T. Kurshan, and A.L. Zimmerman. 2000. *J. Gen. Phys.* 116:755–768; in this issue). Here, we report that a point mutation at position 204 in the S2–S3 loop of Rolf and a mouse CNG channel (Molf) found in olfactory epithelium and heart, increased DAG sensitivity to that of the Brod channel. Mutation of this residue from the wild-type glycine to a glutamate (Molf G204E) or aspartate (Molf G204D) gave dramatic increases in DAG sensitivity without changing the apparent cGMP or cAMP affinities or efficacies. However, unlike the wild-type olfactory channels, these mutants demonstrated voltage-dependent gating with obvious activation and deactivation kinetics. Interestingly, the mutants were also more sensitive to inhibition by the local anesthetic, tetracaine. Replacement of the position 204 glycine with a tryptophan residue (Rolf G204W) not only gave voltage-dependent gating and an increased sensitivity to DAG and tetracaine, but also showed reduced apparent agonist affinity and cAMP efficacy. Sequence comparisons show that the glycine at position 204 in the S2–S3 loop is highly conserved, and our findings indicate that its alteration can have critical consequences for channel gating and inhibition.

KEY WORDS: rod • olfactory • heart • diacylglycerol • tetracaine

INTRODUCTION

Cyclic nucleotide–gated (CNG)[1] cation channels are best characterized in the visual and olfactory systems, but they are also present in tissues as diverse as the heart (Biel et al., 1993; Ruiz et al., 1996), brain (Kingston et al., 1996; Bradley et al., 1997), and kidney (Biel et al., 1994; Karlson et al., 1995). These channels (for reviews see Kaupp, 1995; Molday and Hsu, 1995; Yau and Chen, 1995; Zimmerman, 1995; Finn et al., 1996; Zagotta and Siegelbaum, 1996; Wei et al., 1998; Broillet and Firestein, 1999) are activated by carboxyl-terminal binding of cGMP or cAMP, and most are nonselective cation channels that regulate the membrane potential and Ca^{2+} influx. Other cellular factors modulate the apparent affinity of the channels for cyclic nucleotides and may be involved in regulating physiological responses. These modulators include the following: phosphorylation enzymes (Gordon et al., 1992; Molokanova et al., 1997; Muller et al., 1998), calcium/calmodulin (Hsu and Molday, 1993; Chen and Yau, 1994; Gordon et al., 1995b); and lipids, including diacylglycerol (DAG; Gordon et al., 1995a; Womack et al., 2000).

The I_h channel in the sinoatrial node of the heart controls the pacemaking activity of the heart and is regulated by the binding of cAMP (DiFrancesco and Tortora, 1991). Another CNG channel, found to be diffusely spread throughout the mouse heart, is identical to the mouse olfactory (Molf) CNG channel, but its function in the heart remains unknown (Ruiz et al., 1996). As sensors of cyclic nucleotide concentrations and conduits for Ca^{2+} entry, these CNG channels may also play a role in regulating the heart rate and contraction.

We had previously shown that DAG reversibly inhibits the native rod channel without a phosphorylation reaction as if by direct interaction with some site on the channel (Gordon et al., 1995a). In the companion paper (Crary et al., 2000, in this issue), we discovered that the DAG sensitivities of the Brod and Rolf cloned channels are quite different. In addition, using chimeras of these two channels, we found that the transmembrane segments S2–S6 and their connecting loops seem to be implicated in the differential responses to the inhibitor. In comparison, the amino and carboxyl termini were less critical determinants of the different responses to DAG.

Several studies have highlighted key regions that influence channel gating. These include the amino and carboxyl termini, which have been proposed to interact during gating, as well as the C-linker, which is located

Address correspondence to Anita L. Zimmerman, Department of Molecular Pharmacology, Physiology and Biotechnology, Box G-B329, Brown University, Providence, RI 02912. Fax: (401) 863-1222; E-mail: anita_zimmerman@brown.edu

[1]*Abbreviations used in this paper:* Brod, bovine rod; CNG, cyclic nucleotide–gated; DAG, diacylglycerol; Molf, mouse olfactory; Rolf, rat olfactory.

between the last transmembrane segment and the cyclic nucleotide binding domain and may function as a sensor of the binding event that triggers the allosteric opening transition of the channel (Zong et al., 1998; Paoletti et al., 1999). Other regions thought to be involved in gating are the pore region (Bucossi et al., 1996) and the latter portion of the amino terminus through the S2–S3 loop (Goulding et al., 1994). Using chimeras of Brod and Rolf CNG channels, Gordon and Zagotta (1995) found that control of the apparent cGMP affinity was distributed diffusely throughout the channel protein. All of this information has yet to be assembled into a unified picture of channel gating.

While exploring the mechanism of inhibition by the local anesthetic, tetracaine, Fodor et al. (1997) used a series of Brod and Rolf chimeras to demonstrate an inverse relationship between the $K_{1/2}$ for activation by cGMP and the IC_{50} for inhibition by tetracaine. This finding predicts that channels that are very sensitive to tetracaine should have relatively low apparent affinities for cyclic nucleotides, and is consistent with their general conclusion that tetracaine stabilizes the closed state of the channel. However, we have found that Molf G204E, Rolf G204E, and Rolf G204D, when compared with wild-type olfactory channels, show a marked increase in inhibition by tetracaine, as well as by DAG, without a significant change in $K_{1/2}$ values for activation by cGMP. However, we did detect changes in voltage dependence and gating kinetics, suggesting that mutations at position 204 do affect gating, and that these parameters are more sensitive indicators of channel gating than are equilibrium parameters such as $K_{1/2}$. These results are supported by findings with a mutant containing a tryptophan at position 204 (Rolf G204W). Interestingly, this mutant channel is not only very sensitive to DAG and tetracaine, but it also shows voltage dependence and pronounced gating kinetics, as well as lower apparent agonist affinity and cAMP efficacy.

MATERIALS AND METHODS

Mutagenesis and Expression of Channels by Xenopus Oocytes

The plasmids containing the α subunits of Brod (CNG1) and Rolf (CNG2) cDNA were generous gifts from W.N. Zagotta (University of Washington, Seattle, WA) and the mouse olfactory (Molf G204E) clone was provided by M.L. Ruiz (Entelos, Inc., Menlo Park, CA) (Ruiz et al., 1996). For alternative terminology of the channels, see Richards and Gordon (2000). All vectors and procedures for oocyte preparation and cRNA transcription are described in the companion article (Crary et al., 2000, in this issue).

The primary sequences of the Molf G204E and Rolf clones were aligned for comparison to identify residue differences, and through mutagenesis and functional analysis, we confirmed that the residue at position 204 was responsible for the differential inhibition by DAG reported in this study. Point mutations were incorporated using either the Transformer™ site-directed mutagenesis kit from CLONTECH Laboratories, Inc. or the QuickChange™ site-directed mutagenesis kit from Stratagene. Both kits allow mutagenesis in our high expression vector without subcloning. The mutagenic primers were designed to encode the desired mutation and its surrounding sequence in which we also incorporated a restriction enzyme site (for initial screening purposes) without altering the primary sequence of the protein. For the conversion of the Molf G204E to wild-type Molf, the restriction enzyme site that had been introduced during cloning (SacI) was removed to convert the glutamate residue at position 204 to glycine, which was reported in the genomic sequence (Ruiz et al., 1996). Aside from position 204, the Molf clone sequence differed from the Rolf sequence by 11 amino acids. To eliminate these differences from the study, the glycine residue at position 204 in the Rolf channel was replaced with glutamate (E), aspartate (D), tryptophan (W), and lysine (K). However, Rolf G204K did not give functional expression in our studies. All mutant constructs were subjected to DNA sequencing to confirm the desired sequences.

Electrophysiological Methods

All experiments were performed on inside-out membrane patches excised from *Xenopus* oocytes that were expressing α homomultimers of one of the wild-type or mutant channel types. The cell chamber in which patches were excised consisted of a petri dish containing 15 ml of solution with or without saturating concentrations of cGMP. The solution compositions and method of application are as described in the companion article (Crary et al., 2000, in this issue).

Patch-clamp electrodes were prepared from borosilicate glass capillaries with openings that ranged from 0.5 to 20 μm in diameter, producing resistances of 0.6–15 MΩ. Patches were typically excised in low divalent sodium solutions containing saturating concentrations of cGMP (2 mM for Brod channels and 100 μM for Molf and Rolf channels). A low divalent sodium solution without cGMP was applied as a control to measure the resulting leak current which was subtracted from experimental measurements to obtain the cyclic nucleotide–activated current. We monitored the patch for ~10–40 min, until patch responses to low agonist concentrations stabilized, to ensure that any spontaneous changes in channel behavior, such as those caused by dephosphorylation (Gordon et al., 1992; Molokanova et al., 1997), had occurred before the addition of DAG to the bathing solution. Therefore, none of these changes would be confused with the effects of DAG. Once responses to low cGMP became consistent, we typically measured the patch current produced in response to ranges of cGMP and/or cAMP concentrations to produce dose–response curves before adding DAG.

Patch-clamp data acquisition and analysis were as described in the companion article (Crary et al., 2000, in this issue). For the analysis of the gating kinetics, the only patches excluded from the study as uninterpretable were those in which: (a) the currents were distorted by large ion depletion effects (Zimmerman et al., 1988); (b) the currents were very small and, therefore, were not easily resolvable over noise; and (c) control (i.e., leak) currents were not stable and/or linear throughout the course of the experiment.

RESULTS

Residue at Position 204 Dictates the Response of Olfactory Channels to DAG

Sequence comparison of the Molf and Rolf clones showed differences at 12 positions throughout the protein, and there were an extra five amino acids located at the carboxyl-terminal tail of the Molf clone. Analysis of the Molf channel cDNA sequence reported in the En-

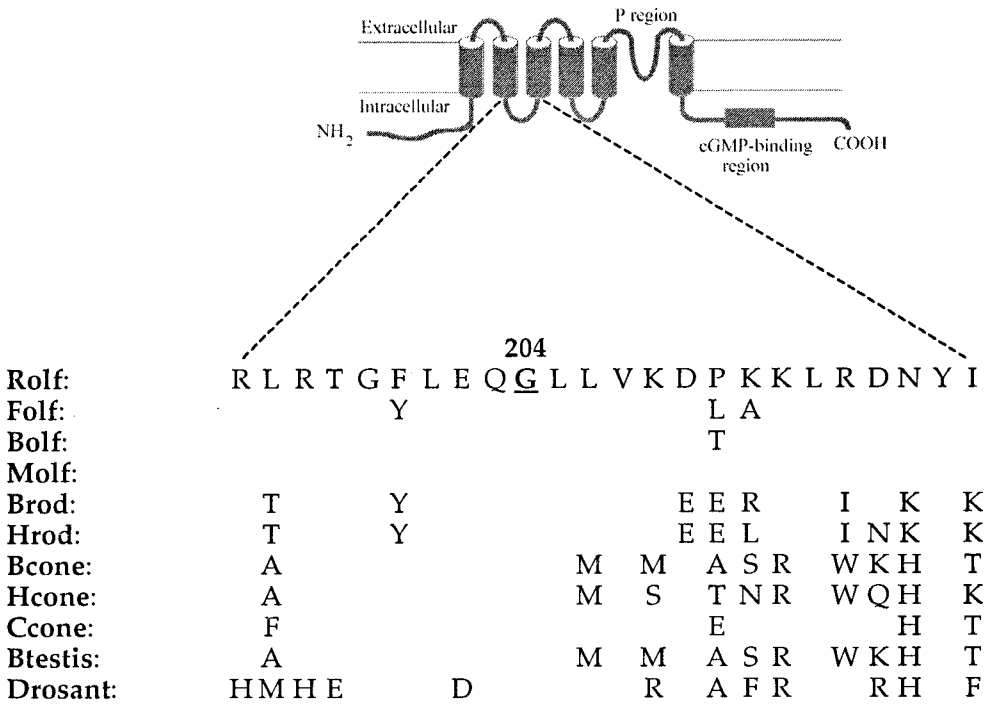

FIGURE 1. Amino acid sequences of the S2–S3 loop of various wild-type CNG channels. Top diagram demonstrates the primary structure and membrane topology of a CNG channel. All wild-type sequences contain a glycine residue at the site equivalent to position 204 (highlighted in bold and underlined) in the Rolf channel. Residues corresponding to the equivalent Rolf residues at positions 199–207 are very highly conserved in all channels. In contrast, there is more variation in the carboxyl-terminal half of the loop sequence. Rolf, rat olfactory; Folf, fish olfactory; Bolf, bovine olfactory; Molf, mouse olfactory; Brod, bovine rod; Hrod, human rod; Bcone, bovine cone; Hcone, human cone; Ccone, chick cone; Btestis, bovine testis; and Drosant, *Drosophila* antenna. The original Molf clone contained a mutation at position 204 (Molf G204E), and we mutated the glutamate (E) to the wild-type glycine (G). For the Rolf channel, the glycine at 204 was replaced with either glutamate, aspartate (D), or tryptophan (W). Replacement with a lysine residue (K) gave no functional expression.

trez database (National Center for Biotechnology Information) revealed that 2 of the 12 changes were introduced with restriction enzyme sites during cloning. The first of these two was a methionine changed to a valine at position 2, and the second was a glycine changed to glutamate at position 204. The other 10 differences appear to be true discrepancies between the Molf and Rolf CNG channels. As will be described in more detail later, the original Molf clone (referred to as Molf G204E) was much more sensitive to DAG than was the wild-type Rolf channel. A concurrent study used chimeras of the Brod and Rolf CNG channels to locate the regions of the Brod channel that could convey the higher sensitivity to DAG; the transmembrane segments and their connecting loops were identified as sensitive regions in the Brod channel (Crary et al., 2000, in this issue). These results led us to investigate the nonconservative substitution at position 204, which is located in the S2–S3 loop (Fig. 1) of the Molf clone.

Site-directed mutagenesis was used to substitute the glutamate residue at this position with the wild-type glycine residue. This construct will be herein referred to as Molf, the true wild-type channel. To eliminate potential effects of the 11 other differences, the glycine at position 204 in the Rolf channel was replaced with a glutamate residue, permitting evaluation of the effect of this isolated point mutation on the DAG sensitivity of the Rolf channel. The requirement of a negative charge in conveying the observed functional changes was tested by substituting another negatively charged residue (aspartate [D]), or a bulky hydrophobic residue (tryptophan [W]). Residue 204 was also replaced by the positively charged residue lysine (K), but we never observed functional expression with this construct. Fig. 1 shows the sequence alignment of 11 homologous CNG channels in the region equivalent to residues 195–218 of the Rolf channel. Notably, the glycine at position 204 is conserved throughout these sequences, including in the Brod channel, which is only 55% identical to the Rolf channel, and must have other differences that cause its relatively high sensitivity to DAG.

Apparent Agonist Affinities and cAMP Efficacies of Molf G204E and Rolf G204E CNG Channels Are Similar to those of Wild-type Molf and Rolf Channels

Dose–response curves for activation by cGMP and cAMP in Fig. 2 demonstrate relative apparent agonist affinities for Brod, Molf, Rolf, Molf G204E, and Rolf G204E CNG homomultimeric (α only) channels. The cGMP dose–response curve for Brod channels is shifted to the right with respect to all other channels shown, indicating its lower apparent affinity for cGMP (Fig. 2 A). Wild-type and mutant (G204E) rat and mouse olfactory channels respond with similar relative apparent affinities for cGMP and cAMP (Fig. 2, A and B). Furthermore, saturating concentrations of both cAMP and cGMP, which act as full agonists, elicit maximal responses from all olfactory channels shown. In contrast, the Brod CNG

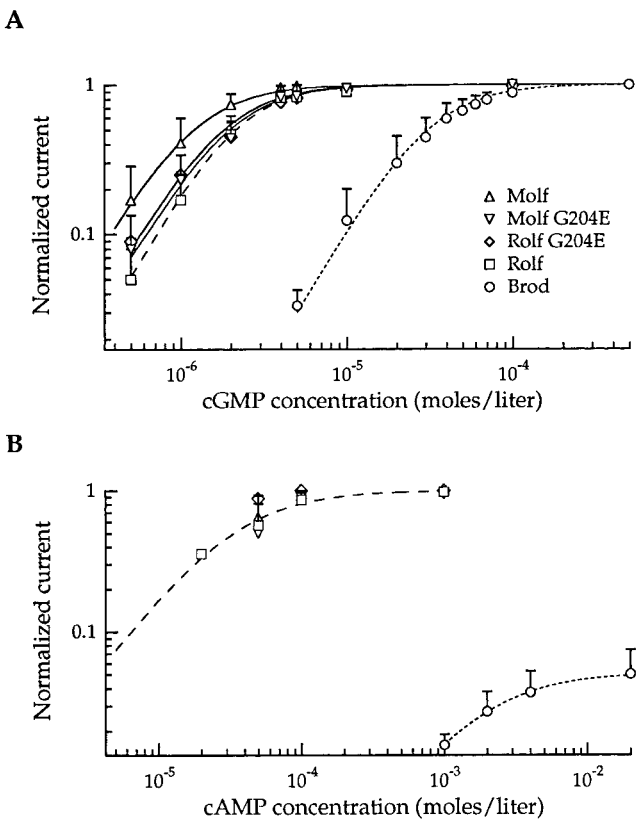

FIGURE 2. Sensitivities to cGMP and cAMP of Molf G204E and Rolf G204E CNG channels were similar to those of the wild-type Molf and Rolf channels. Brod and Rolf data are from the companion article (Crary et al., 2000, in this issue). Steady state, cGMP-activated currents were measured at +100 mV. (A) cGMP dose–response curves for the three wild-type channels, Molf G204E, and Rolf G204E channels. SDs are indicated by error bars. Smooth curves were drawn by fitting the averaged data with the Hill equation, $I/I_{max} = [cNMP]^n/(K_{1/2}{}^n + [cNMP]^n)$, where I is the cGMP- or cAMP-activated current, I_{max} is the cGMP-activated current obtained at saturating cGMP, $K_{1/2}$ is the concentration of cGMP or cAMP giving half-maximal activation, and n is the Hill coefficient. In fitting the data, this relation was scaled to match the measured maximal I/I_{max} (e.g., the maximal I/I_{max} for the rod channel in the presence of saturating cAMP was only 0.05 [B], rather than 1, as for saturating cGMP). The Hill relation was used only for an empirical description of the data to quantify changes in the apparent affinity and maximal activation (or inhibition; see Figs. 4 and 8); it is not meant to suggest a mechanism of channel activation or inhibition by DAG. The calculated $K_{1/2}$ values were 31 μM (Brod; 11 patches), 1.2 μM (Molf; 10 patches), 2.1 μM (Rolf; 18 patches), 1.9 μM (Molf G204E; 8 patches), and 1.8 μM (Rolf G204E; 6 patches). Hill fits for Brod and Rolf channels are designated by dashed lines for emphasis. (A) Dose–response curves for activation by cAMP; the symbols are the same as those used in A. Averaged data points are shown with the SD as error bars: Brod (8 patches), Rolf (7 patches), Molf (5 patches), Rolf G204E (1 patch), and Molf G204E (4 patches). Hill fits to channel data indicate $K_{1/2}$ values for activation by cAMP of 1.83 mM for Brod and 37 μM for Rolf and are represented by dashed lines. See Table I for additional information.

channel responds with a dramatically higher apparent affinity for cGMP than for cAMP, which acts as only a partial agonist of the channel, activating only a fraction (5%) of the current produced by saturating levels of cGMP, even at maximal cAMP concentrations. Therefore, the sequence differences, including the mutation at residue 204, between the Molf G204E and Rolf channels do not significantly affect the apparent agonist affinities or efficacies of the channels. For the Rolf G204D mutant, the responses to cGMP and cAMP are similar to that of Rolf G204E (data not shown).

Brod, Molf G204E, and Rolf G204E Channels Display Higher Sensitivity to DAG than do the Wild-type Molf and Rolf Channels

Application of DAG to the intracellular surfaces of excised patches suppressed current activated by cGMP in all CNG channels studied in the absence of ATP, which indicates that the inhibition does not depend on phosphorylation by PKC. The extent of inhibition by DAG varied according to the concentration of agonist and the channel type. Fig. 3 demonstrates that the addition of DAG produced a greater inhibition of Brod and Molf G204E channels than of Rolf CNG channels. The current traces were recorded for each channel type at saturating cGMP levels in both the presence and absence of DAG. The addition of 1.5 μM DAG had a large effect on both the Brod and Molf G204E channels, decreasing the maximal current by >80% in each case. However, this dose of DAG had a small effect on the Rolf channel, reducing its maximal current by only 14%. As seen with the native rod CNG channel (Gordon et al., 1995a), the suppression of current by DAG was reversible (data not shown) when the bath was diluted by the addition of large volumes of solution containing saturating cGMP without DAG.

To further investigate the differences observed in Fig. 3, we measured DAG dose–response curves for each channel type at saturating concentrations of cGMP. Fig. 4 illustrates that cGMP-activated currents in Brod, Molf G204E, and Rolf G204E channels are fully suppressed by ~3 μM DAG, whereas the cGMP-activated currents of the wild-type Molf and Rolf channels are much less sensitive to the inhibitor, displaying only partial inhibition at 12 μM DAG. Thus, the DAG dose–response relations of Molf G204E and Rolf G204E channels closely resemble those of Brod CNG channels (Fig. 4), even though their apparent affinities for cGMP and cAMP, as well as their cAMP efficacies (Fig. 2), resemble those of the wild-type olfactory channels (summarized in Table I). As discussed later, other gating properties (voltage dependence and kinetics) of these mutant channels were more clearly different from those of the wild-type

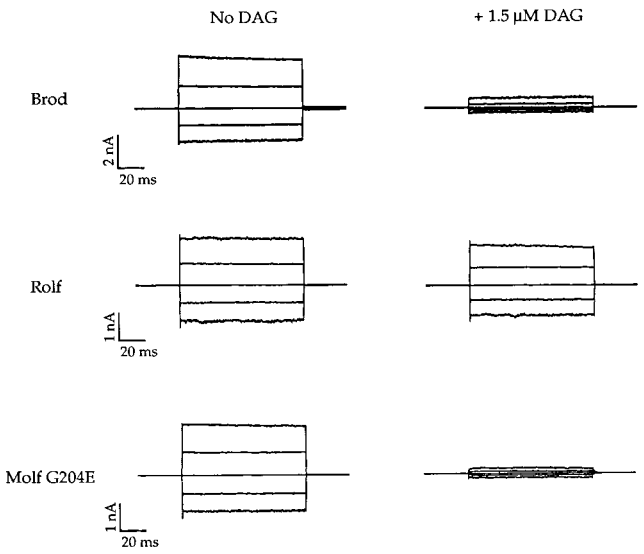

FIGURE 3. Current families from patches at saturating cGMP showed greater inhibition of current by DAG in Molf G204E and Brod channels than in Rolf channels. Current traces were obtained from excised, inside-out patches. Leak currents in the absence of cGMP have been subtracted. Membrane potentials were held at 0 mV and jumped in increments of 50 mV from −100 to +100 mV. The families on the left were obtained at saturating cGMP (2 mM cGMP for Brod and 100 μM for Rolf and Molf G204E), and the families on the right were obtained after the addition of 1.5 μM DAG.

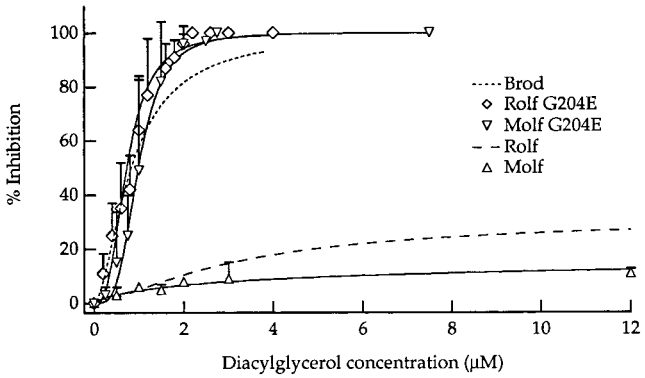

FIGURE 4. DAG completely suppressed saturating cGMP-activated currents of Molf G204E and Rolf G204E CNG channels, but only partially inhibited the corresponding wild-type channels at saturating agonist concentrations. Brod and Rolf data from the companion article (Crary et al., 2000, in this issue) are shown for comparison. Saturating cGMP concentrations were 2 mM for Brod channels and 100 μM for all Molf and Rolf channels. Averaged data obtained at saturating cGMP were fit with the Hill equation, $IN/IN_{max} = [DAG]^n/(IC_{50}{}^n + [DAG]^n)$ where IN is the percent inhibition, IN_{max} is maximal inhibition, IC_{50} is the concentration of DAG required to achieve half-maximal inhibition, and n is the Hill coefficient. As for Fig. 2, the relation was scaled to reflect the measured maximal IN/IN_{max}. For the Brod, Molf G204E, and Rolf G204E channels, the maximum inhibition was 100%. For Brod (11 patches), IC_{50} = 0.83 μM, and n = 1.7; for Molf G204E (12 patches), IC_{50} = 0.99 μM, and n = 3.6; and for Rolf G204E (5 patches), IC_{50} = 0.73 μM and n = 2.8. For the wild-type olfactory channels, inhibition is only partial. For Rolf (13 patches), IN_{max} = 31%, IC_{50} = 3.24 μM (denoting 15.5% inhibition), and n = 1.4; and for Molf (5 patches), IN_{max} = 17%, IC_{50} = 3.50 μM (denoting 8.5% inhibition), and n = 0.8. Hill fits of Brod and Rolf channels are designated by dashed lines. Error bars indicate SDs.

olfactory channels. As expected, the behavior of the Rolf G204D mutant was found to resemble that of Rolf G204E (data not shown).

The Mutant (G204E) Olfactory Channels Show Voltage-dependent Gating Not Observed with Wild-type Olfactory Channels

Since the Molf and Molf G204E channels had very different responses to DAG, it was surprising that our initial measurements of gating by cyclic nucleotides seemed so similar. On closer inspection, we found that, unlike wild-type olfactory channels, the Molf G204E and Rolf G204E channels exhibited prominent voltage-dependent gating kinetics similar to those previously described for the native rod CNG channel (Karpen et al., 1988). The channels are slightly voltage-dependent, with depolarization favoring channel opening. Thus, at positive potentials, the current increases as more channels open, and at negative potentials, the current decreases as channels close. In this study, we specifically looked for similar voltage-dependent gating kinetics. The Brod channel typically shows gating kinetics similar to those in the left panel of Fig. 5. Here, at low [cGMP], a slow rise in the outward current occurs during the time course of positive voltage pulses (activation kinetics), and a slow fall in current occurs during negative voltage pulses (deactivation kinetics). Fig. 5 shows that the Molf channel (middle) has no obvious gating kinetics, whereas Molf G204E (right) has gating kinetics resembling those of the Brod channel (left). The absence of detectable gating kinetics observed for the Molf channel was also observed for the Rolf channel (data not shown). The slight rectification seen in the Molf current family was the same magnitude at all cGMP concentrations, and probably reflects some proton block at pH 7.2 (Root and MacKinnon, 1994; Gavazzo et al., 1997).

We also looked for evidence of voltage-dependent gating by plotting dose–response curves for cGMP at both +100 and −100 mV. Results from multiple patches are shown in Fig. 6 for Brod, Rolf, and Rolf G204E. To control for patch-to-patch variability in the apparent cGMP affinity, all data for each patch were normalized to the $K_{1/2}$ at +100 mV for that patch. For Brod and Rolf G204E, the shift in the data at −100 mV relative to +100 mV indicates voltage-dependent gating. In contrast, the dose–response curves for the Rolf channel did not shift, suggesting that gating of this channel is not voltage-dependent. The ratios of $K_{1/2}$ at

TABLE I

*Summary of Effects of Agonists and Inhibitors on Different Channel Types**

	cGMP	cAMP		DAG		Tetracaine	
Channel	$K_{1/2}$	$K_{1/2}$	Efficacy‡	IC_{50}	Maximal percent inhibition§	IC_{50}‖	Percent inhibition¶
Brod	31.0	1830	0.05	0.83	100	2.6	94.1
Rolf	2.1	37	1	3.24	31	139.6	10.4
Molf	1.2	37	1	3.50	17	–	18.8
Molf G204E	1.9	37	1	0.99	100	10.8	78.3
Rolf G204E	1.8	37	1	0.73	100	–	76.4
Rolf G204W	14.0	440	0.44	0.26	100	2.2	100

*The values for $K_{1/2}$ and IC_{50} were all obtained from Hill fits of averaged data at +100 mV and are expressed in micromolar. All IC_{50} values were obtained with saturating cGMP. Except for tetracaine IC_{50} values (see below), the number of patches used to obtain each value is indicated in the figure legends. For the cAMP $K_{1/2}$ values, the same curve was used to fit data for Rolf, Molf, Molf G204E, and Rolf G204E (Fig. 2 B). ‡The fractional current obtained with saturating cAMP relative to that obtained with saturating cGMP. This value was obtained from the Hill fits that were used to calculate the $K_{1/2}$ for averaged data, except in the case of Rolf G204W, where the efficacy was the average of values obtained at saturating cAMP for two patches. §Maximal percent inhibition at saturating DAG concentrations. This value was obtained from the Hill fits that were used to calculate the IC_{50}. ‖The tetracaine IC_{50} value reported here for Brod was obtained from the literature (Fodor et al., 1997). The tetracaine IC_{50} values for Rolf, Molf G204E, and Rolf G204W were obtained from two, one, and one patch(es), respectively.¶Percent inhibition at 40 μM.

−100 mV to $K_{1/2}$ at +100 mV are 1.4 and 1.7 for the Brod and Rolf G204E channels, respectively.

The Rolf G204W Mutant Demonstrates Decreased Apparent Agonist Affinities and cAMP Efficacy as well as Voltage-Dependent Gating and Higher Sensitivity to DAG

The families of currents in Fig. 7 A reveal observable gating kinetics for the Rolf G204W mutant channel that resemble those seen with the Brod channel but not with the wild-type Rolf channel (Fig. 5). In addition, Fig. 7 (B and C, and Table I) shows that the apparent agonist affinities ($K_{1/2}$ values for cGMP and cAMP) of Rolf G204W are intermediate between those for the Rolf and Brod channels (Fig. 2 and Table I). Similarly, the cAMP efficacy for Rolf G204W lies between that for the Rolf and Brod channels. The points in Fig. 7 B provide cGMP dose–response data at two different voltages (+100 and −100 mV), illustrating the voltage dependence of gating that was observed for the Brod channel but not for the Rolf channel (Fig. 6). Fig. 8 A and Table I indicate that DAG inhibition of the Rolf G204W mutant is even more like that of the Brod channel than are the agonist affinities and efficacies; in fact, the Rolf G204W channel is actually more sensitive to DAG than is the Brod channel. These data show that the introduction of a bulky hydrophobic residue (tryptophan) at position 204 in the Rolf channel has an even greater impact on channel function than the introduction of negatively charged residues. In Fig. 8 B, the current–voltage relation for the Rolf G204W channel again shows the slight voltage dependence of the mutant that is intrinsic to gating. As observed for the Brod and Rolf channels (Crary et. al, 2000, in this issue), the addition of DAG does not introduce any further voltage dependence than that which is expected at lower open probability (Karpen et al., 1988).

Residue 204 Mutants Are Also More Sensitive to Block by Tetracaine

To explore the mechanism by which residue 204 alters DAG sensitivity, we also studied the very different inhibitor, tetracaine. Tetracaine dose–response curves (data not shown), obtained for some of the mutant channels at saturating cGMP concentrations, indicated that the sensitivity to tetracaine (like that to DAG) is much greater for Molf G204E and Rolf G204D (IC_{50} = 10.8 μM for both mutants) than for the Rolf channel (IC_{50} = 139.6 μM). Thus, the response to tetracaine for both mutants was more like that reported for the Brod chan-

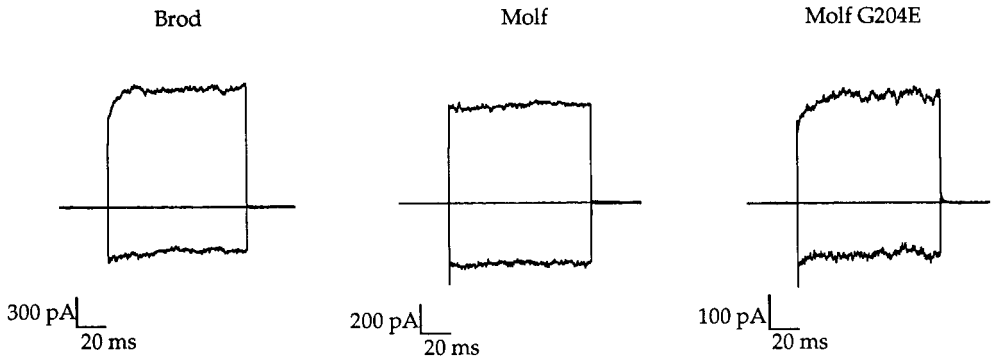

FIGURE 5. A glutamate at position 204 of the Molf or Rolf channel produced gating kinetics similar to those of the Brod channel. In the absence of DAG, the Molf channel has no detectable gating kinetics, whereas Molf G204E has obvious gating kinetics, much like the Brod channel. Currents were obtained with either 10 μM (Brod), 1 μM (Molf), or 1 μM (Molf G204E) cGMP in response to voltage jumps ranging from −100 to +100 mV in steps of 50 mV, from a holding potential of 0 mV. For clarity, only currents at −100, 0, and +100 mV are shown. At +100 mV, the observed currents had an I/I_{max} of 0.20, 0.15, and 0.15, respectively (from left to right).

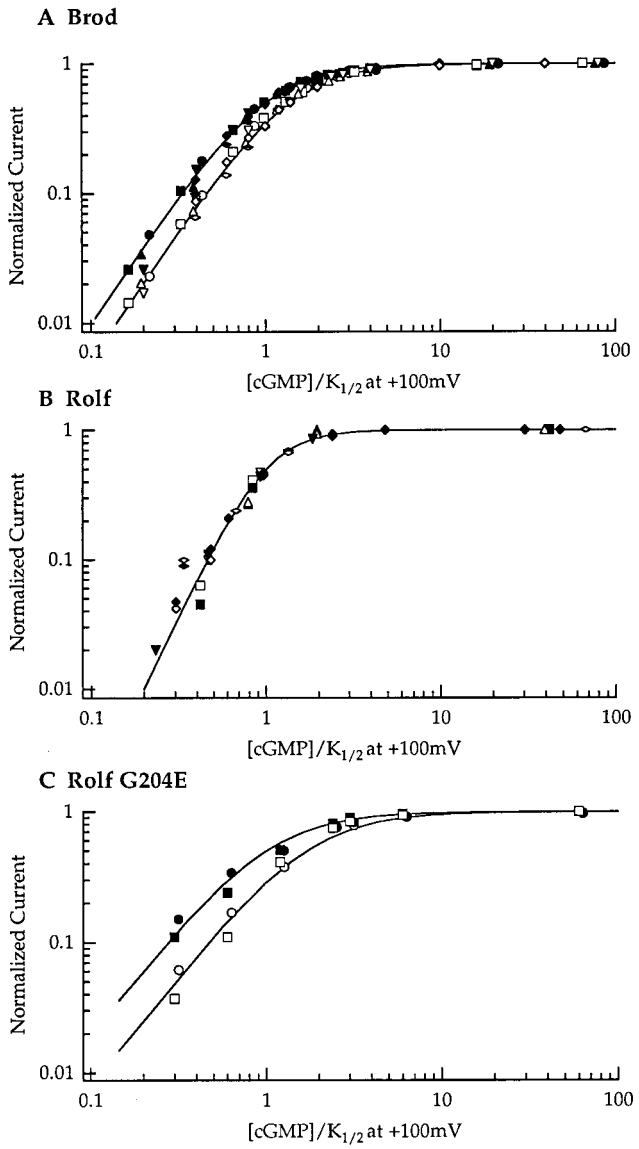

FIGURE 6. A glutamate at position 204 of the Molf or Rolf channel produced voltage-dependent gating similar to that of the Brod channel. To analyze the data from multiple patches, the dose–response curve from each patch was fit with the Hill relation, and each set of data was normalized to the cGMP $K_{1/2}$ at +100 mV for that patch. Each different symbol represents the normalized data points from a single patch; open symbols for −100 mV and closed symbols for +100 mV. All points for each voltage were re-fit with the Hill equation, setting the normalized $K_{1/2}$ for +100 mV at 1.0; a change in the normalized $K_{1/2}$ at −100 mV indicates voltage-dependent gating. (A) Brod channel (six patches): at +100 mV, n = 2.0; and at −100 mV, the normalized cGMP $K_{1/2}$ = 1.4 and n = 2.0. (B) Rolf channel (six patches): at +100 mV, n = 2.8; and at −100 mV, the normalized cGMP $K_{1/2}$ = 1.0 and n = 2.8. (C) Rolf G204E channel (2 patches): at +100 mV, n = 1.7; and at −100 mV, the normalized cGMP $K_{1/2}$ = 1.7 and n = 1.7.

nel (IC_{50} = 2.6 μM; Fodor et al., 1997) than that of the Rolf channel. Fig. 9 and Table I summarize the responses of all channel types to tetracaine at saturating cGMP concentrations (2 mM cGMP for all channels). The percent inhibition by 40 μM tetracaine was four- to eightfold greater for the three mutants than for their wild-type counterparts. As found for DAG inhibition, Rolf G204W behaved similarly to the Brod channel with respect to tetracaine inhibition: it was 100% inhibited (without deviation) at 40 μM tetracaine.

DISCUSSION

We have identified a residue in the S2–S3 loop that is highly conserved among the CNG channel family members, and that influences channel gating and inhibition by DAG and tetracaine. Replacement of the glycine at position 204 of the mouse or rat olfactory channel with a negatively charged residue (glutamate or aspartate) created channels with dramatically increased sensitivity to both DAG and tetracaine but a less obvious change in channel gating. These mutations introduced voltage dependence and gating kinetics without a change in apparent agonist affinity or efficacy. However, substitution of residue 204 with tryptophan resulted in more dramatic effects on gating as well as higher sensitivity to the two inhibitors. In fact, unlike the other mutants, the tryptophan mutant demonstrated a decrease in apparent agonist affinity and cAMP efficacy, in addition to the appearance of voltage-dependent gating. These results indicate that it is not merely the charge of the glutamate and aspartate residues that altered channel gating and inhibitor sensitivities; instead, the mutations may have changed the secondary structure or simply the flexibility of the loop region by introducing bulkier groups than the wild-type glycine. Alternatively, the replacement of glycine at position 204 may have changed the nature of interactions of this loop with other parts of the channel. The Hill coefficients from the DAG dose–response curves of the more sensitive channels confirm that at least two or three molecules of DAG are typically required to inhibit a channel (discussed in more detail in the companion article Crary et al., 2000, in this issue). This is in contrast to inhibition by tetracaine in which one molecule appears to block the closed pore of the channel (Fodor et al., 1997). Consistent with our results with the rod and olfactory channels (see Crary et al., 2000, in this issue), inhibition of the mutant channels by DAG does not appear to be voltage-dependent, but, as expected, the voltage dependence of gating becomes more evident upon stabilization of the closed state(s) by DAG.

The Molf G204E, Rolf G204E, and Rolf G204D constructs provide the first demonstration of a point mutation that drastically alters inhibition by DAG or tetracaine without altering the apparent sensitivity to cyclic nucleotides. How could a change in the residue at position 204 have a similar dramatic effect on inhibition by two structurally different inhibitors without changing these gating parameters? Our results suggest that gating

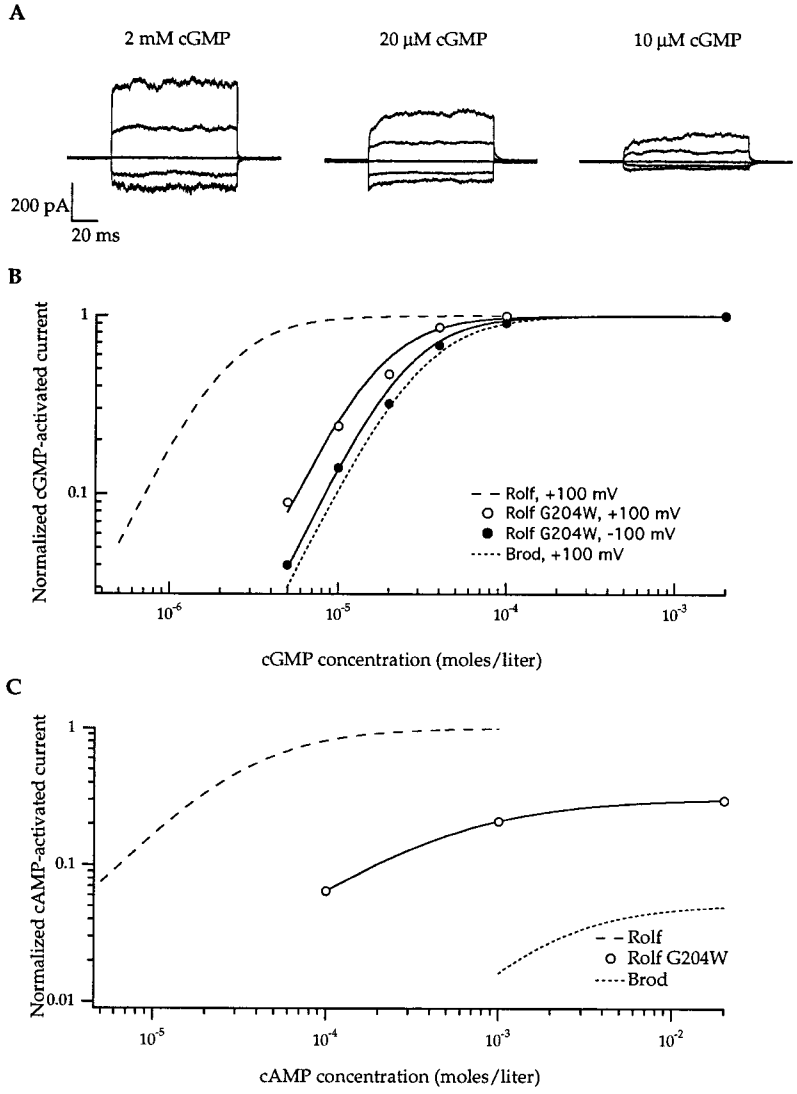

FIGURE 7. Introduction of tryptophan at position 204 produced a mutant Rolf channel with measurable gating kinetics, lower apparent agonist affinity, and decreased cAMP efficacy. (A) The current families were obtained with the designated amounts of cGMP in response to voltage jumps ranging from −100 to +100 mV in 50-mV steps, from a holding potential of 0 mV. The traces were corrected for leak by subtracting responses in the absence of cGMP. (B) The dose–response curves for activation by cGMP at + 100 mV and −100 mV are shown for a single patch containing the Rolf G204W mutant; the data were fit with the Hill relation, as in Fig. 2 (see legend). For this patch, at +100 mV, the cGMP $K_{1/2}$ = 14 μM and n = 2.0; and at −100 mV, the cGMP $K_{1/2}$ = 18 μM and n = 2.0. For averaged data from six patches, at +100 mV, the $K_{1/2}$ = 14 μM and n = 1.7; and at −100 mV, the $K_{1/2}$ = 19 μM and n = 1.7. The Hill fits (Fig. 2) for the cGMP dose–response curves of the Rolf and Brod channels (at +100 mV) are shown for comparison. (C) cAMP is only a partial agonist for Rolf G204W, unlike the Rolf channel (Hill fit from Fig. 2 is shown for comparison). A dose–response curve for activation by cAMP is shown for a single patch: $K_{1/2}$ = 440 μM and n = 0.9. The average efficacy for two patches was 44%.

kinetics are more sensitive to changes in the allosteric conformational change than are standard equilibrium gating parameters such as apparent cGMP affinity and cAMP efficacy. Thus, unlike the wild-type olfactory channel, the aspartate and glutamate mutants demonstrated voltage-dependent gating kinetics, resembling those previously documented for the native rod CNG channel (Karpen et al., 1988). We have not seen similar gating kinetics with the wild-type olfactory channels, but we have seen them with the cloned rod channel as well as with the position 204 mutants (glutamate and aspartate).

The voltage dependence was further investigated by plotting the dose–response curves at +100 and −100 mV. As expected, a shift between these dose–response curves was observed for the Brod and Rolf G204E channels, but not for the Rolf channel. These studies, demonstrating weakly voltage-dependent gating, are consistent with previous findings for Brod α homomultimers (Benndorf et al., 1999) as well as those for the native CNG channel (Karpen et al., 1988). However, one study reported voltage dependence in the Brod heteromultimers (α and β subunits), but not in the Brod α homomultimeric channels (Shammat and Gordon, 1999). The lack of voltage dependence in the Rolf α homomultimers is consistent with the studies by Bradley et al. (1994) and Liman and Buck (1994).

Although the introduction of a negative charge at position 204 produced only subtle changes in gating properties, the substitution of a bulky hydrophobic group (tryptophan) had more severe consequences. Interestingly, this single point mutation converted the olfactory channel to one that behaves more like the rod channel, displaying lower apparent agonist affinity, cAMP efficacy, as well as more pronounced gating kinetics and voltage dependence. In light of the drastically altered gating properties of the Rolf G204W mutant, it is not surprising that its response to inhibitors is also like that of the rod channel. One possible explana-

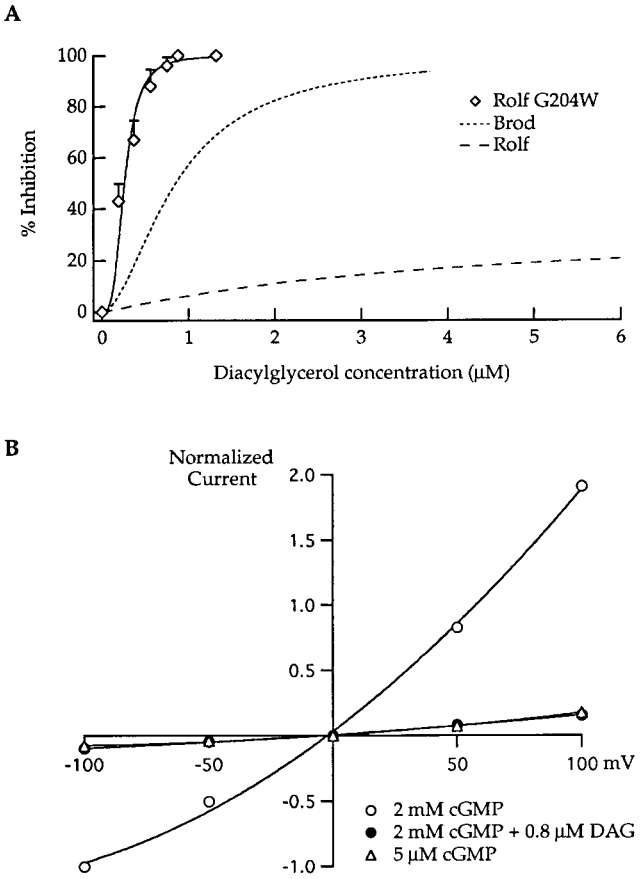

FIGURE 8. The Rolf G204W mutant had a slightly greater DAG sensitivity than that of the Brod channel, and its inhibition was similarly voltage-independent (compare with Fig. 4 in companion article, Crary et al., 2000, in this issue). (A) The DAG dose–response curve was measured in the presence of 2 mM cGMP: data were averaged from three patches and fit with the Hill equation. The maximum inhibition for the Rolf G204W mutant was 100% with an IC_{50} = 0.26 μM and n = 3.2. The Hill fits for the Brod and Rolf channels (from Fig. 4) are shown for comparison as dashed curves. (B) Steady state current–voltage relations obtained from data acquired on a single patch containing the Rolf G204W mutant. Open circles represent cGMP-activated currents at saturating concentrations in the absence of DAG. Filled circles represent currents at saturating cGMP in the presence of 0.8 μM DAG. For comparison, the triangles show the currents at lower (5 μM) cGMP concentration, without DAG.

tion for the larger effect of the tryptophan molecule on channel gating is that its hydrophobic side chain may insert into the bilayer and disrupt the normal motions of the transmembrane segments that occur during allosteric transitions, in much the same way as we have proposed for the DAG molecule (see first model of Fig. 10 in companion article, Crary et al., 2000, in this issue). Alternatively, the tryptophan may produce larger effects on gating than glutamate or aspartate simply because it has a different effect on the secondary structure of the region.

Since glycine is present at the equivalent of position 204 in both the rod and olfactory channels (Fig. 1), other residue differences between the two channels must be responsible for the differential DAG inhibition of these two channels. In fact, a parallel study with chimeras of the two channels demonstrated that regions outside of the S2–S3 loop of the rod channel can also convey DAG sensitivity (see companion article Crary et al., 2000, in this issue). Thus, there is no clear evidence as to whether this loop constitutes a DAG binding site; instead, it may play a critical role in gating, such that structural alterations may result in functional modifications that also render the channel more sensitive to closed state inhibitors. Chimera studies previously have shown that swapping S2 and the adjoining S2–S3 loop of bovine rod and catfish olfactory channels had only moderate effects on ligand sensitivity or efficacy (Goulding et al., 1994); yet, this loop is part of a larger region, including the latter part of the amino terminus, that has been found to affect gating when the entire region is swapped. Swapping the amino-terminal part alone gave only moderate effects. Therefore, it is possible that a nonconservative residue difference in the S2–S3 loop of the rod channel may also contribute to the differences in gating and sensitivity to inhibitors of the two different channels. Further studies are required to elucidate the role of the loop in the mechanism(s) of channel gating and DAG inhibition.

In the lac permease of *Escherichia coli*, deletions in the loops were generally not disruptive to the protein's function unless they encroached on the boundaries with the transmembrane segments, where critical residues were proposed to actually be part of the transmembrane helix (Wolin and Kaback, 1999). Thus, in the case of Rolf G204W, it is somewhat surprising that a point mutation in the putative middle of the S2–S3 loop of the Rolf CNG channel alters channel behavior so dramatically. Interestingly, mutation of a histidine residue in the same loop of the KAT1 channel recently has been shown to affect activation kinetics and pH dependence (Tang et al., 2000). It is possible that the wild-type S2–S3 loop has a very distinct interaction with another part of the CNG channel, and is, therefore, directly involved in the normal allosteric transition(s) that occur during channel gating. Alternatively, the loop may simply be a hinge that maintains a particular distance between (or alignment of) the transmembrane segments that compose the core of the channel. A similar purpose has been proposed for the loops in ligand-gated ion channel receptors (Lynch et al., 1997). The structure of such a hinge may determine its flexibility, which may be critical during the conformational changes that constitute channel gating, a process that most likely requires movement of the transmembrane segments in the membrane as proposed for

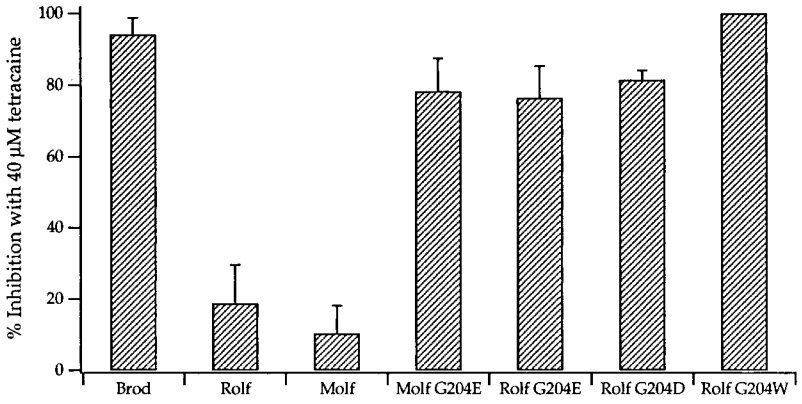

FIGURE 9. All mutant olfactory channels had greater sensitivity to tetracaine than did the wild-type olfactory channels. Averaged data are reported for percent inhibition at 40 μM tetracaine for Brod (3 patches), Rolf (10 patches), Molf (5 patches), Molf G204E (4 patches), Rolf G204E (4 patches), Rolf G204D (2 patches), and Rolf G204W (4 patches). SDs are indicated by error bars. Values of percent inhibition are found in Table I.

other channels (Unwin, 1995; Perozo et al., 1999). Evidence from work on homologous K^+ channels suggests that the S2 transmembrane segment may participate in channel gating via a charge interaction with the S4 segment (Papazian et al., 1995; Seoh et al., 1996; Monks et al., 1999; Milligan and Wray, 2000). Thus, structural changes in the attached loops may disrupt coordinated movements of these two transmembrane segments, thereby altering channel gating properties, including voltage dependence. Our results indicate that the highly conserved glycine at position 204 in the S2–S3 loop of the CNG channels may be critical for maintaining a particular structure that is involved in the normal gating mechanism in wild-type channels.

We are grateful to Drs. Sharona Gordon and Gary Yellen for helpful discussions, and Dr. William N. Zagotta for comments on an earlier version of the manuscript. We thank Dr. Maria Ruiz for the mouse olfactory clone and Dr. William N. Zagotta for the bovine rod and rat olfactory constructs. We also thank Elizabeth Seed, Wang Nguitragool, and Roberto Neisa for their technical assistance.

This work was supported by the American Heart Association of Rhode Island (grant No. 97-07721S) and the National Institutes of Health (grant No. EY07774).

Submitted: 10 May 2000
Revised: 22 September 2000
Accepted: 2 October 2000

REFERENCES

Benndorf, K., R. Koopman, E. Eismann, and U.B. Kaupp. 1999. Gating by cyclic GMP and voltage in the α subunit of the cyclic GMP-gated channel from rod photoreceptors. *J. Gen. Phys.* 114: 477–489.

Biel, M., W. Altenhofen, R. Hullin, J. Ludwig, M. Freichel, V. Flockerzi, N. Dascal, U.B. Kaupp, and F. Hofmann. 1993. Primary structure and functional expression of a cyclic nucleotide-gated channel from rabbit aorta. *FEBS Lett.* 329:134–138.

Biel, M., X. Zong, M. Distler, E. Bosse, N. Klugbauer, M. Murakami, V. Flockerzi, and F. Hofmann. 1994. Another member of the cyclic nucleotide-gated channel family, expressed in testis, kidney, and heart. *Proc. Natl. Acad. Sci. USA.* 91:3505–3509.

Bradley, J., J. Li, N. Davidson, H.A. Lester, and K. Zinn. 1994. Heteromeric olfactory cyclic nucleotide-gated channels: a subunit that confers increased sensitivity to cAMP. *Proc. Natl. Acad. Sci. USA.* 91:8890–8894.

Bradley, J., Y. Zhang, R. Bakin, H.A. Lester, G.V. Ronnett, and K. Zinn. 1997. Functional expression of the heteromeric "olfactory" cyclic nucleotide-gated channel in the hippocampus: a potential effector of synaptic plasticity in brain neurons. *J. Neurosci.* 17: 1993–2005.

Broillet, M.C., and S. Firestein. 1999. Cyclic nucleotide-gated channels. Molecular mechanisms of activation. *Annu. NY Acad. Sci.* 868:730–740.

Bucossi, G., E. Eismann, F. Sesti, M. Nizzari, M. Seri, U.B. Kaupp, and V. Torre. 1996. Time-dependent current decline in cyclic GMP-gated bovine channels caused by point mutations in the pore region expressed in *Xenopus* oocytes. *J. Physiol.* 493.2:409–418.

Chen, T.-Y., and K.-W. Yau. 1994. Direct modulation by Ca^{2+}-calmodulin of cyclic nucleotide-activated channel of rat olfactory receptor neurons. *Nature.* 368:545–548.

Crary, J.I., D.M. Dean, W. Nguitragool, P.T. Kurshan, and A.L. Zimmerman. 2000. Mechanism of inhibition of cyclic nucleotide-gated ion channels by diacylglycerol. *J. Gen. Phys.* 116:755–768.

DiFrancesco, D., and P. Tortora. 1991. Direct activation of cardiac pacemaker channels by intracellular cyclic AMP. *Nature.* 351:145–147.

Finn, J.T., M.E. Grunwald, and K.-W. Yau. 1996. Cyclic nucleotide-gated ion channels: an extended family with diverse functions. *Annu. Rev. Physiol.* 58:395–426.

Fodor, A.A., S.E. Gordon, and W.N. Zagotta. 1997. Mechanism of tetracaine block of cyclic nucleotide-gated channels. *J. Gen. Phys.* 109:3–14.

Gavazzo, P., C. Picco, and A. Menini. 1997. Mechanisms of modulation by internal protons of cyclic nucleotide-gated channels cloned from sensory receptor cells. *Proc. R. Soc. Lond. B. Biol. Sci.* 264:1157–1165.

Gordon, S.E., and W.N. Zagotta. 1995. Localization of regions affecting an allosteric transition in cyclic nucleotide-activated channels. *Neuron.* 14:857–864.

Gordon, S.E., D.L. Brautigan, and A.L. Zimmerman. 1992. Protein phosphatases modulate the apparent agonist affinity of the light-regulated ion channel in retinal rods. *Neuron.* 9:739–748.

Gordon, S.E., J. Downing-Park, B. Tam, and A.L. Zimmerman. 1995a. Diacylglycerol analogs inhibit the rod cGMP-gated channel by a phosphorylation-independent mechanism. *Biophys. J.* 69: 409–417.

Gordon, S.E., J. Downing-Park, and A.L. Zimmerman. 1995b. Modulation of the cGMP-gated ion channel in frog rods by calmodulin and an endogenous inhibitory factor. *J. Physiol.* 486:533–546.

Goulding, E.H., G.R. Tibbs, and S.A. Siegelbaum. 1994. Molecular mechanism of cyclic-nucleotide-gated channel activation. *Nature.* 372:369–374.

Hsu, Y.-T., and R.S. Molday. 1993. Modulation of the cGMP-gated channel of rod photoreceptor cells by calmodulin. *Nature.* 361: 76–79.

Karlson, K.H., F. Ciampolillo-Bates, D.E. McCoy, N.L. Kizer, and B.A. Stanton. 1995. Cloning of a cGMP-gated cation channel from mouse kidney inner medullary collecting duct. *Biochim. Biophys. Acta.* 1236:197–200.

Karpen, J.W., A.L. Zimmerman, L. Stryer, and D.A. Baylor. 1988. Gating kinetics of the cyclic-GMP-activated channel of retinal rods: flash photolysis and voltage-jump studies. *Proc. Natl. Acad. Sci. USA.* 85:1287–1291.

Kaupp, U.B. 1995. Family of cyclic nucleotide gated ion channels. *Curr. Opin. Neurobiol.* 5:434–442.

Kingston, P.A., F. Zufall, and C.J. Barnstable. 1996. Rat hippocampal neurons express genes for both retinal and olfactory cyclic nucleotide-gated channels: novel targets for cAMP/cGMP function. *Proc. Natl. Acad. Sci. USA.* 93:10440–10445.

Liman, E.R., and L.B. Buck. 1994. A second subunit of the olfactory cyclic nucleotide-gated channel confers high sensitivity to cAMP. *Neuron.* 13:611–621.

Lynch, J.W., S. Rajendra, K.D. Pierce, C.A. Handford, P.H. Barry, and P.R. Schofield. 1997. Identification of intracellular and extracellular domains mediating signal transduction in the inhibitory glycine receptor chloride channel. *EMBO (Eur. Mol. Biol. Organ.) J.* 16:110–120.

Milligan, C.J., and D. Wray. 2000. Local movement in the S2 region of the voltage-gated potassium channel hKv2.1 studied using cysteine mutagenesis. *Biophys. J.* 78:1852–1861.

Molday, R.S., and Y.-T. Hsu. 1995. The cGMP-gated channel of photoreceptor cells: its structural properties and role in phototransduction. *Behav. Brain Sci.* 18:441–451.

Molokanova, E., B. Trivedi, A. Savchenko, and R.H. Kramer. 1997. Modulation of rod photoreceptor cyclic nucleotide-gated channels by tyrosine phosphorylation. *J. Neurosci.* 17:9068–9076.

Monks, S.A., D.J. Needleman, and C. Miller. 1999. Helical structure and packing orientation of the S2 segment in the *Shaker* K^+ channel. *J. Gen. Phys.* 113:415–423.

Muller, F., W. Bönigk, F. Sesti, and S. Frings. 1998. Phosphorylation of mammalian olfactory cyclic nucleotide-gated channels increases ligand sensitivity. *J. Neurosci.* 18:164–173.

Paoletti, P., E. Young, and S.A. Siegelbaum. 1999. C-linker of cyclic nucleotide–gated channels controls coupling of ligand binding to channel gating. *J. Gen. Phys.* 113:17–33.

Papazian, D.M., X.M. Shao, S.A. Seoh, A.F. Mock, Y. Huang, and D.H. Wainstock. 1995. Electrostatic interactions of S4 voltage sensor in *Shaker* K^+ channel. *Neuron.* 14:1293–1301.

Perozo, E., D.M. Cortes, and L.G. Cuello. 1999. Structural rearrangements underlying K^+-channel activation gating. *Science.* 285:59–61.

Richards, M.J., and S.E. Gordon. 2000. Cooperativity and cooperation in cyclic nucleotide-gated ion channels. *Biochemistry.* In press.

Root, M.J., and R. MacKinnon. 1994. Two identical noninteracting sites in an ion channel revealed by proton transfer. *Science.* 265: 1852–1856.

Ruiz, M.L., B. London, and B. Nadal-Ginard. 1996. Cloning and characterization of an olfactory cyclic nucleotide-gated channel expressed in mouse heart. *J. Mol. Cardiol.* 28:1453–1461.

Seoh, S.-A., D. Sigg, D.M. Papazian, and F. Bezanilla. 1996. Voltage-sensing residues in the S2 and S4 segments of the *Shaker* K^+ channel. *Neuron.* 16:1159–1167.

Shammat, I.M., and S.E. Gordon. 1999. Stoichiometry and arrangement of subunits in rod cyclic nucleotide-gated channels. *Neuron.* 23:809–819.

Tang, X.D., I. Marten, P. Dietrich, N. Ivashikina, R. Hedrich, and T. Hoshi. 2000. Histidine^{118} in the S2-S3 linker specifically controls activation of the KAT1 channel expressed in *Xenopus* oocytes. *Biophys. J.* 78:1255–1269.

Unwin, N. 1995. Acetylcholine receptor channel imaged in the open state. *Nature.* 373:37–43.

Wei, J.-Y., D.S. Roy, L. Leconte, and C.J. Barnstable. 1998. Molecular and pharmacological analysis of cyclic nucleotide-gated channel function in the central nervous system. *Prog. Neurobiol.* 56:37–64.

Wolin, C.D., and H.R. Kaback. 1999. Estimating loop-helix interfaces in a polytopic membrane protein by deletion analysis. *Biochemistry.* 38:8590–8597.

Womack, K.B., S.E. Gordon, F. He, T.G. Wensel, C.C. Lu, and D.W. Hilgemann. 2000. Do phosphatidylinositides modulate vertebrate phototransduction? *J. Neurosci.* 20:2792–2799.

Yau, K.-W., and T.Y. Chen. 1995. Cyclic nucleotide-gated channels. *In* Handbook of Receptors and Channels: Ligand and Voltage-gated Ion Channels. R.A. North, editor. CRC Press, Boca Raton, FL. pp. 307–335.

Zagotta, W.N., and S.A. Siegelbaum. 1996. Structure and function of cyclic nucleotide-gated channels. *Annu. Rev. Neurosci.* 19:235–263.

Zimmerman, A.L. 1995. Cyclic nucleotide gated ion channels. *Curr. Opin. Neurobiol.* 5:296–303.

Zimmerman, A.L., J.W. Karpen, and D.A. Baylor. 1988. Hindered diffusion in excised patches from retinal rod outer segments. *Biophys. J.* 54:351–355.

Zong, X., H. Zucker, F. Hofmann, and M. Biel. 1998. Three amino acids in the C-linker are major determinants of gating in cyclic nucleotide-gated channels. *EMBO (Eur. Mol. Biol. Organ.) J.* 17: 353–362.